Journal of Advanced Research in Fluid Mechanics and Thermal Sciences

Journal homepage:
https://semarakilmu.com.my/journals/index.php/fluid_mechanics_thermal_sciences/index
ISSN: 2289-7879

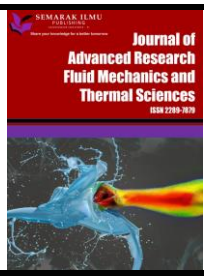

Numerical Analysis of Recycled AA6061 Reinforced Alumina Oxide Undergoing Finite Strain Deformation Uniaxial Tensile and Taylor Cylinder Impact Tests

Norzarina Ma'at[1], Mohd Khir Mohd Nor[1,*]

[1] Crashworthiness and Collision Research Group (COLORED), Faculty of Mechanical and Manufacturing Engineering, Universiti Tun Hussein Onn Malaysia, Parit Raja, Batu Pahat, 86400, Johor, Malaysia

ARTICLE INFO

Article history:
Received 18 May 2023
Received in revised form 26 July 2023
Accepted 5 August 2023
Available online 19 August 2023

Keywords:
Recycled Aluminium Alloy Reinforced Alumina Oxide (Al_2O_3); Finite Element Analysis; LS-DYNA

ABSTRACT

Recycling aluminum is a topic of high interest due to the global demand for aluminum-based products. This approach presents a great opportunity to address the environmental issues caused by the primary production of aluminum made from bauxite ore. In recent years, many researchers have explored the recycling of aluminum alloys, including reinforcement, to achieve better results and improve properties. However, there have been limited efforts to predict the deformation behaviour of such materials numerically. It is generally agreed that advancements in numerical analysis are important to accelerate progress and establish the application of newly developed materials. Therefore, this study aimed to numerically predict the deformation behaviour of recycled aluminum alloy AA6061 reinforced with Alumina Oxide, subjected to finite strain deformation of uniaxial tensile tests at different strain rates (6x10-1s-1 to 6x10-3s-1) and Taylor Cylinder Impact at different impact velocities (190ms-1 to 370ms-1) using the LS-DYNA simulation code. In this numerical analysis, a Simplified Johnson-Cook model is adopted and characterized. The simulation results, which were validated against published experimental data, showed good agreement, establishing appropriate numerical prediction capabilities for recycled aluminum alloys AA6061 reinforced with Alumina Oxide.

1. Introduction

Solid waste in Malaysia is a hot topic due to the rapid growth of the local population and high daily consumption [1,2]. Therefore, many researchers are focused on exploring recycling and sustainability issues to reduce waste, address environmental problems, and find recyclable materials that have the potential for various applications.

The usage of aluminum alloy has experienced rapid growth every year in various industrial sectors due to its excellent properties. However, the production of aluminum, including bauxite mining, requires high energy consumption, which can have environmental impacts. Therefore, secondary

* *Corresponding author.*
E-mail address: khir@uthm.edu.my

https://doi.org/10.37934/arfmts.108.2.6276

production through aluminum recycling is being used to meet demands while preserving the environment as mention by Rahim *et al.,* [3]. Aluminum recycling demonstrates a positive trend as awareness of environmentally preferred products increases. It can be observed that a majority of aluminum products in the European Union are made from recycled raw materials Tillová *et al.,* [4].

Recycling aluminium can save energy and reduce the use of natural resources. According to Subodh *et al.,* [5], recycled aluminium is more economical and environmentally friendly compared to primary aluminium. Primary aluminium production requires 45 kWh/kg of metal produced, whereas secondary aluminium made from recycled materials only needs 2.8 kWh/kg of metal produced. The energy savings amounted to approximately 1.72×1011 kWh per year in 2003.

Aluminium matrix composite (AMC) is a globally recognized material widely employed in various sectors [6-11]. This material is commonly used as a critical component in the automotive and aerospace industries. Generally, AMC consists of lightweight aluminium alloys reinforced with non-metallic particles (hard ceramics) such as Silicon Carbide (SiC), Alumina Oxide (Al_2O_3), and Boron Carbide (B_4C). AMC offers high specific modulus, strength, lightweight properties, strong wear resistance, and low thermal expansion. Alumina Oxide (Al_2O_3) is commonly used as a reinforcement due to its excellent combination with aluminium alloys. Alumina is chemically inert and can withstand higher temperatures compared to unreinforced aluminium alloys. The addition of alumina particles helps improve the mechanical properties of the composite [6-8]. Alumina significantly enhances the strength of the composite; however, it may reduce ductility and elongation due to its ceramic properties, which can lead to specimen fracture during necking.

Numerous researchers have made significant efforts to study the strain-rate dependency of materials, and it has been observed that different materials exhibit varying behaviors under different strain rates [12-16]. However, when it comes to characterizing materials undergoing finite strain deformation, the focus has predominantly been on primary aluminum alloys [17-22].

Recently, Ho *et al.,* [23] examined the strain rate effects of recycled aluminium alloy AA6061 through uniaxial tensile testing. The observations revealed that the mechanical response of recycled aluminium alloy AA6061 improved as the strain rate increased. In another study by Ho *et al.,* [24], a Taylor cylinder aluminium alloy impact test was conducted at higher strain rate levels to investigate the deformation behaviour of recycled aluminium alloy AA6061 at various impact velocities. The results showed that the recycled aluminium alloy AA6061 exhibited a non-symmetric ellipse-shaped footprint with mushrooming, tensile splitting, and petalling fracture modes, indicating anisotropic deformation behavior. Additionally, the recycled aluminium alloy AA6061 displayed a ductile fracture mode and a strong strain rate dependency, with increasing impact velocity leading to higher levels of damage evolution.

Ma'at *et al.,* [25] characterized the deformation behaviour of recycled aluminium alloy reinforced with alumina oxide in terms of mechanical properties, damage progression, and fracture mode using the uniaxial tensile test. The results indicate that increasing the strain rate leads to an increase in the number of voids. Overall, the recycled aluminium alloy AA6061 reinforced with alumina oxide exhibits a strain-rate-dependent behaviour. They also investigated the deformation behaviour and fracture mode of recycled aluminium alloy AA6061 reinforced with alumina oxide at a high strain rate using the Taylor cylinder impact test [26]. Within the impact velocity range of 190-370 m/s, three different fracture modes (mushrooming, tensile splitting, and petalling) were observed. The reinforced recycled aluminium alloy AA6061 showed better strength performance with a higher critical impact velocity than the non-reinforced recycled aluminium alloy AA6061. In terms of damage deformation behaviour, the results showed that the damage agents were initiated, grew, and coalesced during mild ductility deformation. The observation of damage progression revealed that the increment in void size was more significant under tensile splitting and petalling fracture modes

compared to mushrooming, due to severe localized plastic strain deformation around the plastic deformation zone. Therefore, increasing impact velocity increases the severity of the damage progression in the reinforced recycled aluminium alloy AA6061.

Due to the revolution and innovation in technology, numerical analysis is widely used in various designs and applications as an alternative to complex experimental analysis. It helps reduce costs, increase efficiency, and improve the quality of the final product. In addition, numerical analysis provides precise and simplified analysis to verify, understand, and communicate information effectively. It also offers benefits to materials in different system configurations [27,28]. The constitutive model can be accessed by considering material parameters and loading conditions [29-31]. There are numerous simulation tools available with various capabilities for finite element analysis, such as LS-DYNA, ABAQUS, SOLIDWORKS, ANSYS, and others. LS-DYNA is one of the most widely used simulation technologies in the automobile industry for crash simulation [32-34].

The Simplified Johnson-Cook model in LS-DYNA has been widely used in industrial simulations. It provides reasonably good results and is numerically efficient Murugesan *et al.,* [35]. Many researchers [35-39] have performed finite element analyses using the Simplified Johnson-Cook model. From observations, the simulation results show a good agreement with the experimental data, demonstrating the capabilities of this model in predicting material deformation. Therefore, the Simplified Johnson-Cook model is used in this numerical work to predict the deformation of recycled aluminium alloy AA6061 reinforced with alumina oxide.

Moreover, there are numerous computer codes and constitutive models available for primary aluminum alloys that have been extensively utilized by researchers [35-43]. However, no attempts have been made to model the material behaviour of recycled aluminum alloy reinforced with alumina oxide. Based on this motivation, this paper presents a numerical prediction of the deformation behaviour of recycled aluminium alloy AA6061 reinforced with alumina oxide.

2. Methodology

This study was conducted to numerically predict the deformation behaviour of recycled aluminium alloy AA6061 reinforced with alumina oxide undergoing finite strain deformation using LS-DYNA. The deformation behaviour was predicted using both uniaxial tensile tests at lower strain rate levels [25] and Taylor Cylinder impact tests at higher strain rate levels [26]. The Simplified Johnson-Cook model, adopted in this numerical work, was characterized using experimental data from Ma'at *et al.,* [25].

2.1 Finite Element Model

The finite element model used in this study was based on the actual experimental specimens, specifically the ASTM-E8 dog-bone shape and solid cylindrical shape [25,26]. The model was meshed using the Hypermesh software with a 3D solid mapping method and an element size of 0.5 mm. After completing the meshing work, boundary conditions were assigned to the model in the LS-Prepost software, which included constraints, loads, temperature, and material models.

As illustrated in Figure 1, the finite element model is divided into three major parts for the uniaxial tensile test, and the unit system used is mm-s-tonne-N (length-time-mass-force). The first part is configured as a fixed constraint region with no translational or rotational motions during deformation. The second part is the moving constraint region, where a force is applied, and there are no translational or rotational movements along the y and z axes. Finally, the third section is known as the deformation region.

While for the Taylor cylinder impact test, the cm-g-s (length-gravity-time) system of units was used in this simulation. First, the loading condition was applied to the cylinder specimen, with the front face of the cylinder specimen in contact with a target plate. Then, following the experimental setup, the cylinder specimen was launched at an impact velocity of 190-358 m/s to strike the fixed target, as shown in Figure 2. This computer simulation depicts the interaction of reflected compressive and lateral release waves in a cylindrical Taylor specimen subjected to a target plate, resulting in tensile stresses. Additionally, tension is observed due to lateral release, and these tensile stresses can lead to fracturing. In this study, the gravitational effect was ignored.

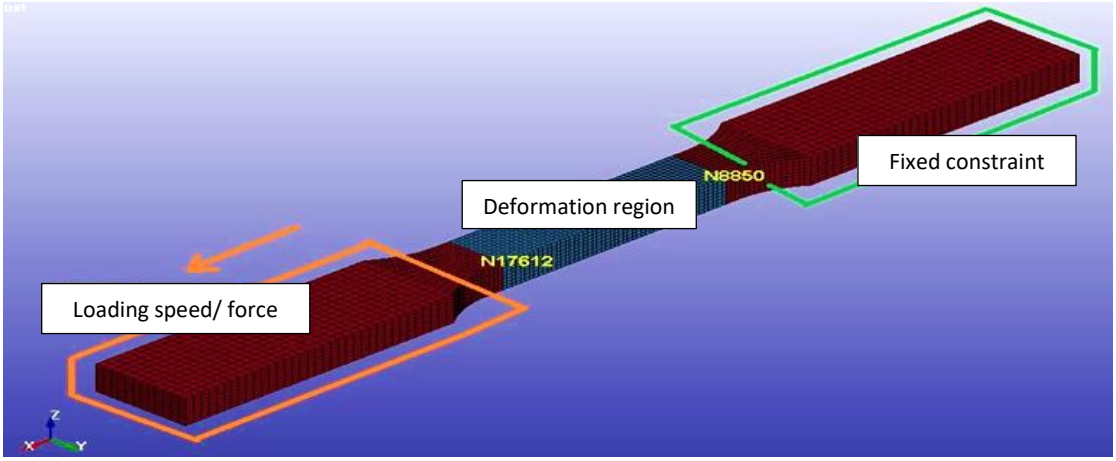

Fig. 1. Finite Element Model of uniaxial tensile test

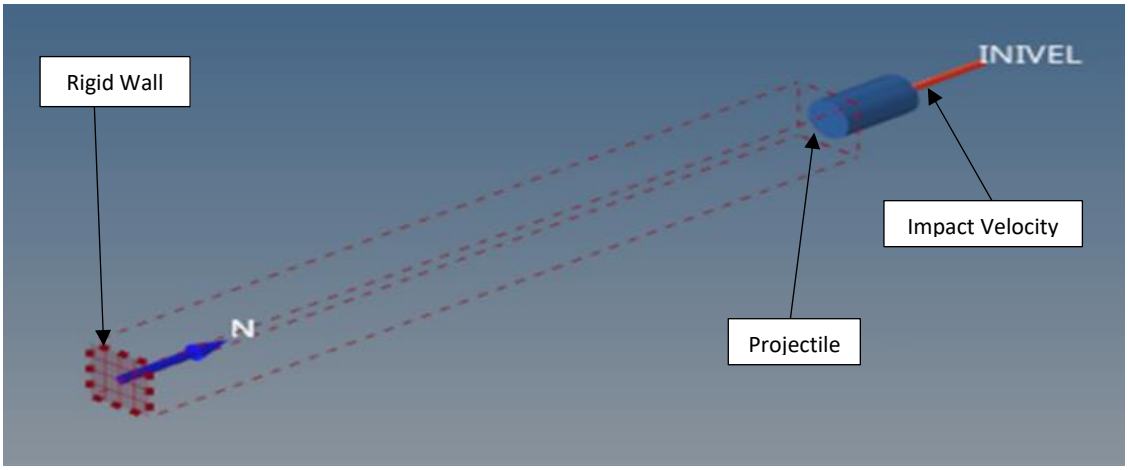

Fig. 2. Finite Element Model of Taylor cylinder impact test

2.2 Input Parameters Characterization of the Johnson-Cook Model

In this research work, the input parameters of the Simplified Johnson-Cook model were derived using experimental data from the uniaxial tensile test. The Johnson-Cook model is defined by Eq. (1). The reference strain rate ($\dot{\varepsilon}_0$) was set as 6×10^{-3} s^{-1} for room temperatures. At the reference strain rate, the strain rate hardening functions are equal to unity. Consequently, the flow stress is given by:

$$\sigma_{eq}\left(\dot{\varepsilon} = \dot{\varepsilon}_{ref}\right) = \left[A + B\varepsilon_{pl}^{n}\right][1 + C\ln 1] = [A + B\varepsilon_{pl}^{n}] \quad (1)$$

This study computed the material constants using the nonlinear solver function in Microsoft Excel. The average engineering stress-strain curve was converted into an actual stress-strain curve.

The elastic part of this curve was removed to obtain the equivalent plastic stress-strain curve, as depicted in Figure 3. The parameter A corresponds to the yield stress (stress at zero plastic strain). To determine B and n, Eq. (1) was fitted to the equivalent plastic stress-strain curve. As this curve is nonlinear, the Generalized Reduced Gradient (GRG) algorithm of the nonlinear solver function in Excel was utilized, as shown in Figure 4. The parameters A, B, and n were then identified and summarized in Table 1.

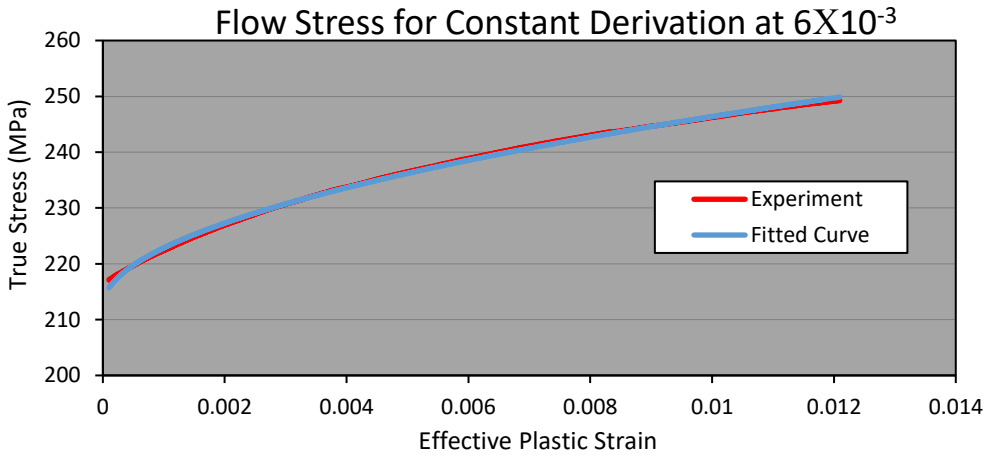

Fig. 3. Flow Stress for constant derivation (*A, B* and *n*) at strain rate: 6×10^{-3} s^{-1}

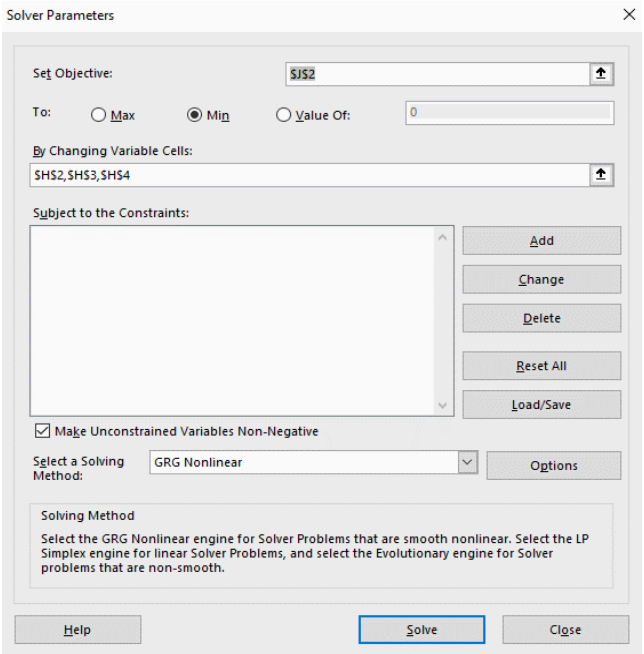

Fig. 4. Excel Solver Function

Table 1
Simplified Johnson-Cook Parameter (A, B and n)

Strain rate, $\dot{\varepsilon}$ (s^{-1})	Yield Strength, A (MPa)	Strain Hardening, B (MPa)	Strain Hardening Exponent, n
6×10^{-3}	212.5223	363.7547	0.5155815
6×10^{-2}	219.2889	483.9896	0.596607
6×10^{-1}	222.3201	334.0997	0.487127

After deriving the values of A, B, and n, the next step was to define the constant C, which controls the strain rate effect. Eq. (1) was once again utilized and rearranged. The true flow stress against the normalized strain rate curve for constant C was then compared with the reference strain rate, as shown in Figures 5 ($6\times10^{-3}s^{-1}$ compared to $6\times10^{-2}s^{-1}$) and Figure 6 ($6\times10^{-3}s^{-1}$ compared to $6\times10^{-1}s^{-1}$). Furthermore, the sum of squared errors method was used to calculate the squared deviation of each data point, which were then summed. Once again, the nonlinear solver function was employed. The material constants C were calculated and are presented in Table 2.

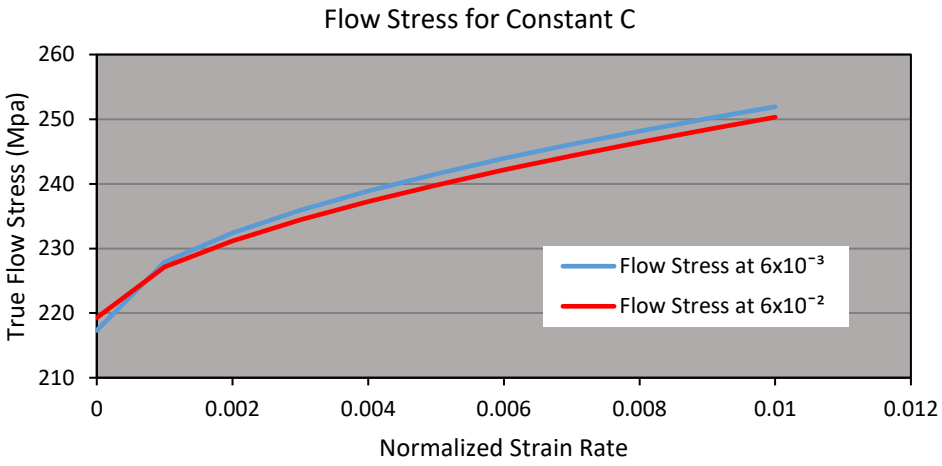

Fig. 5. Flow stress for the constants derivation (*C*) ($6\times10^{-3}s^{-1}$ against $6\times10^{-2}s^{-1}$)

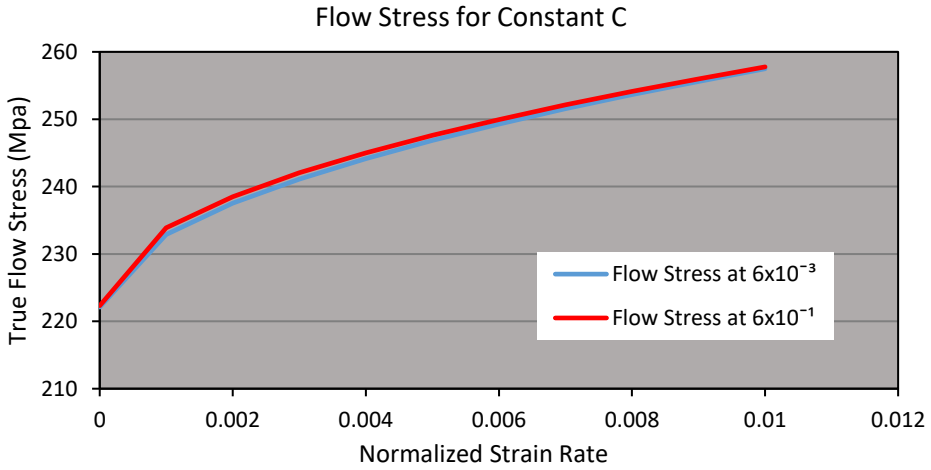

Fig. 6. Flow stress for the constants derivation (*C*) ($6\times10^{-3}s^{-1}$ against $6\times10^{-1}s^{-1}$)

Table 2
Parameter Simplified Johnson-Cook model A, B, n and C

Yield Strength, *A* (MPa)	Strain Hardening, *B* (MPa)	Strain Hardening Exponent, n	Strain Rate Constant, *C*
212.5223	363.7547	0.5155815	0.0098

2.3 Numerical Analysis of Uniaxial Tensile Test

In this section, simulation results are validated against experimental data obtained from uniaxial tensile tests at strain rates of $6\times10^{-3}s^{-1}$, $6\times10^{-2}s^{-1}$, and $6\times10^{-1}s^{-1}$. LS -Prepost was used to extract the simulation results. The stress-strain curves for each uniaxial tensile test at different strain rates were plotted and compared with the experimental data of Ma'at *et al.,* [25] (see Figure 7 to 9). The simulation results are shown by the red line, while the experimental results are shown by the blue line. From the simulation results, as shown in the Figure 7 to 9, it can be noticed that the flow stress of simulation result showed a good match compared with experiment data.

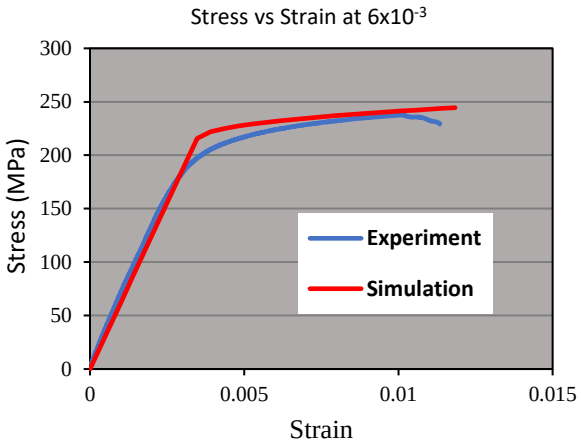

Fig. 7. Simulation result of strain rate 6×10^{-3}

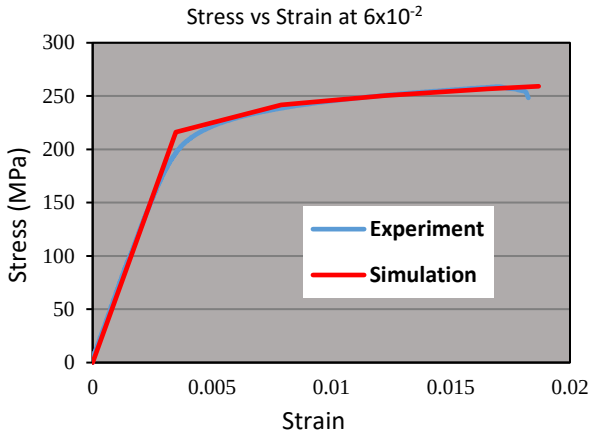

Fig. 8. Simulation result of strain rate 6×10^{-2}

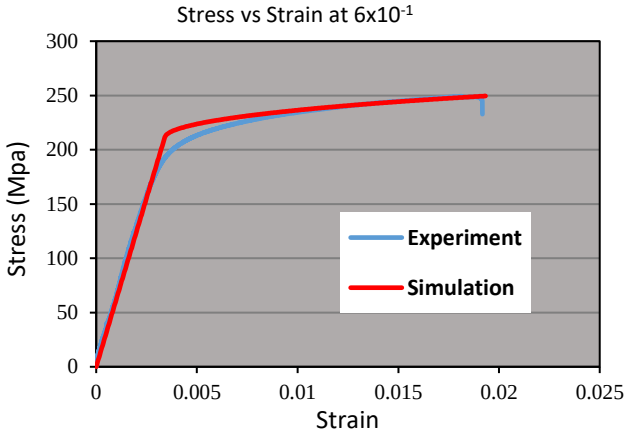

Fig. 9. Simulation Result of Strain Rate 6×10^{-1}

Table 3 summarises the comparison between the simulation and experimental results. The simulation results show that the Simplified Johnson-Cook model using the derived input parameters can effectively predict the elastoplastic deformation behaviour of recycled aluminium alloy AA6061 reinforced with alumina oxide.

Regarding the yield stress values, the simulation results show good agreement with the experimental data, especially with respect to the elastic slope. Minor deviations in the plastic region are still considered acceptable. Furthermore, the simulation values for the modulus of elasticity agree with the experimental data in each test, with differences ranging from 0.05 to 1.43 GPa, or about 0.02% to 2.37% in terms of percentage error.

Simulation results for yield strength also agree well with experimental values, with differences ranging from 7.43 to 11.61 MPa and a percent error of about 4.38% to 5.22%. Although a slight difference between the simulation and experimental results is observed for tensile strength, with differences ranging from 2 to 10.2 MPa and a percent error of 0.78% to 4.34%, these differences remain acceptable. In addition, the total percent errors for the yield stress and ultimate tensile strength were less than 6%, which is generally considered acceptable with a percent error of less than 10%. Therefore, the simulation results for flow stress slightly underestimated the experimental results.

In summary, the Simplified Johnson-Cook model (MAT 98) successfully predicts the deformation behaviour of recycled aluminium alloy AA6061 reinforced with alumina oxide from the quasi-static to intermediated strain rate in uniaxial tensile tests. The simulation results show good agreement with the experimental results.

Table 3
Summary of the Simulation Data and the Experimental Data

Strain rate, (s^{-1})	Data	Young's Modulus, E (GPa)	Yield Strength, σ (MPa)	Ultimate Tensile Strength, UTS (MPa)
6×10^{-3}	Experiment	61.79	221.82	234.80
	Simulation	60.359	212.52	245.00
	Percentage error (%)	2.37	4.38	4.34
6×10^{-2}	Experiment	62.80	226.72	235.29
	Simulation	62.381	219.29	245.1738
	Percentage error (%)	0.67	4.76	4.20
6×10^{-1}	Experiment	63.56	233.93	254.44
	Simulation	63.575	222.32	256.433
	Percentage error (%)	0.02	5.22	0.78

2.3 Numerical Analysis of Taylor Cylinder Impact Test

Few fracture modes were observed in the Taylor cylinder impact specimens that were affected by damage initiation and progression, especially for fracture modes beyond a mushroom shape. It should be noted that the Simplified Johnson-Cook model cannot predict deformation-induced damage. Therefore, its predictions are only applicable to mushroom-shaped deformations. The lack of relevant experimental data makes it impossible to characterise damage-based constitutive models for such recycled materials.

Therefore, in this analysis, the same Simplified Johnson-Cook model as in the previous study was used to predict the deformation of Taylor cylindrical impact specimens that exhibited mushroom-shaped fracture mode. For specimens that exhibited tensile splitting and petalling fracture modes, the damage parameters of the Johnson-Cook model were used. In this analysis, it was assumed that the damage parameters of the primary aluminium alloy AA6061 are also applicable to its counterpart in recycled form, since the mechanical parameters in the elastoplastic range of these materials do not differ significantly. Table 4 shows the mechanical properties of the recycled aluminium alloy AA6061 reinforced with alumina oxide, while Table 5 presents the Johnson Cook damage parameters of the primary aluminium alloy AA6061.

Table 4
Mechanical Properties of Recycled aluminium alloy AA6061 Reinforced Alumina Oxide

Strain rates, $\dot{\varepsilon}$ (s^{-1})	Yield strength, σ_Y (MPa)	Ultimate tensile strength, σ_{UTS} (MPa)	Elastic modulus, E (GPa)	Poisson Ratio, *v*
6×10^{-3}	221.82	234.80	61.79	
6×10^{-2}	226.72	235.29	62.80	0.33
6×10^{-1}	233.93	254.44	63.56	

Table 5
Johnson-Cook Damage Parameters of Primary aluminium alloy AA6061 Sohail *et al.,* [44]

D1	D2	D3	D4	D5	T_0 (°k)
-0.77	1.45	-0.47	0.0	1.6	298

2.3.1 Simulation results and analysis

Figure 10 shows the three fracture modes predicted by the numerical model. Overall, the numerical model succeeds in capturing the fracture modes "mushrooming, tensile splitting, and petalling fracture modes," which are very similar to the experimental results. The simulation accurately reproduces the identical deformation patterns of radial expansion around the footprint and length reduction of the projectile.

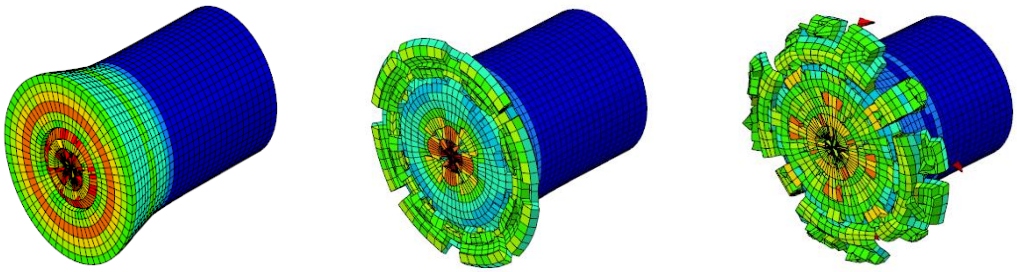

(a) (b) (c)

Fig. 10. Fracture Modes Predicted by the Numerical Model (a) Mushrooming, (b) Tensile Splitting (c) Petalling

Figure 11 to 13 show the simulation footprint, including a comparison with experimental results [23] for different fracture modes. The numerical model agrees with the experimental observations for the analysis of lower impact velocities for fracture modes beyond a mushroom shape. However, the model cannot predict a better fracture mode for the critical impact velocity. Therefore, the numerical model using damage parameters of the primary aluminium alloy AA6061 was used to predict the other fracture mode observed in the experiment. Observation showed that the fracture mode obtained from this simulation was in better agreement with the experimental data than the conventional numerical model. It also showed the predictive ability of this model.

Simulation results for impact velocities from 191 m/s to 231 m/s show a mushroom-shaped fracture mode consistent with the experimental observations shown in Figure 11. However, if the impact velocity exceeds the critical threshold (280 m/s), the numerical results are overestimated compared to the experiment, but with a similar radial expansion, as shown in Figure 12 for the tensile splitting fracture mode (280 m/s to 295 m/s). The simulation results produce excessive cracks and fragments, which is physically unrealistic.

As shown in Figure 13, the simulation results agree with the experimental results for impact velocities from 313 m/s to 322 m/s. However, for impact velocities between 334 m/s and 358 m/s, the simulation results are lower than the experimental values. Overall, the comparison of the results shows that the Simplified Johnson-Cook including damage models are suitable criteria for predicting deformation behaviour, damage, and fracture at impact and high strain rates.

Table 6 compares the simulation and experimental results [23] of the Taylor impact test in terms of final length and diameter after impact. The table shows that the percentage difference between the simulation and experimental results is minimal, with a percentage error of less than 10%, which is considered acceptable. However, at impact velocities of 280ms-1 (tensile splitting), 334ms-1, and 358ms-1 (petalling), the errors were 11%, 11.65%, and 11.09%, respectively, indicating an overestimation of the final diameter of the specimen. In addition, the recycled aluminium alloy AA6061 reinforced with alumina exhibits anisotropic behaviour. The post-test footprint was distorted in different directions and showed a non-symmetrical footprint. As the impact velocity increases, the final length decreases and the final diameter of the specimen increases. The simulation results are in agreement with the experimental results and show a similar trend, which confirms their acceptability.

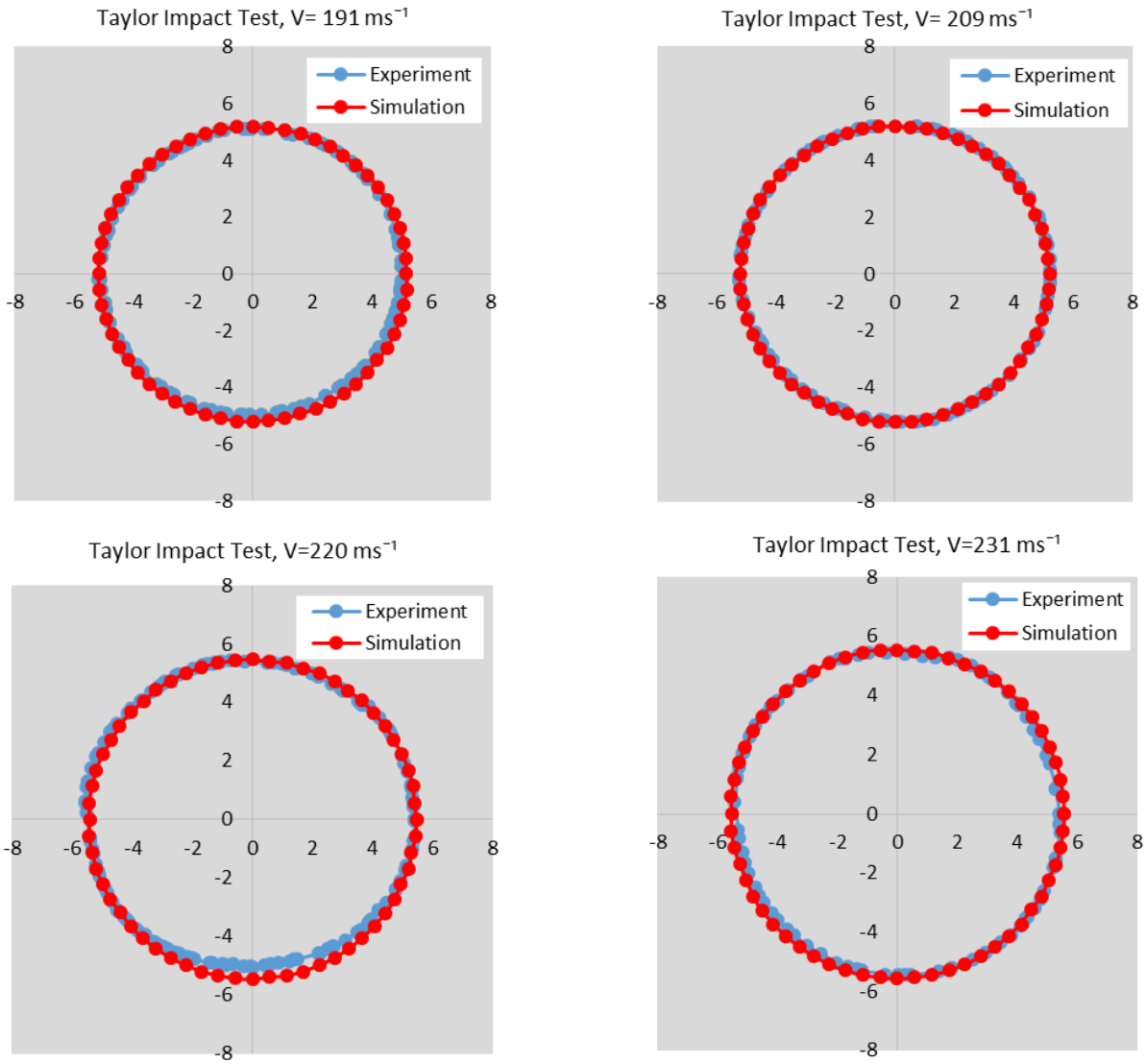

Fig. 11. Simulation of the Mushrooming Fracture Mode

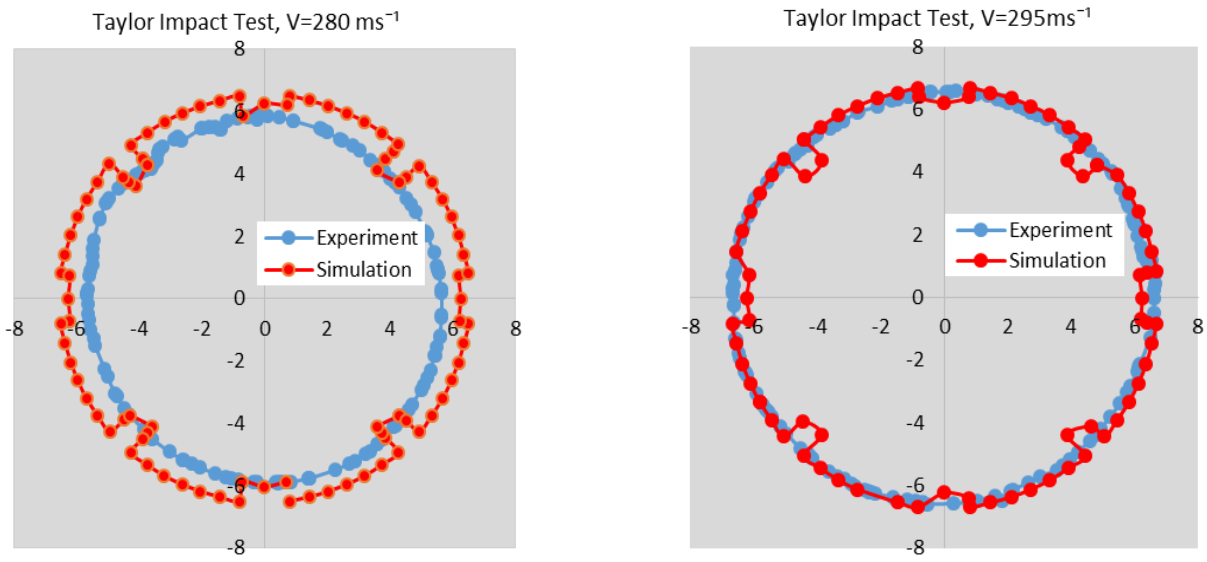

Fig. 12. Simulation of the Tensile Splitting Fracture Mode

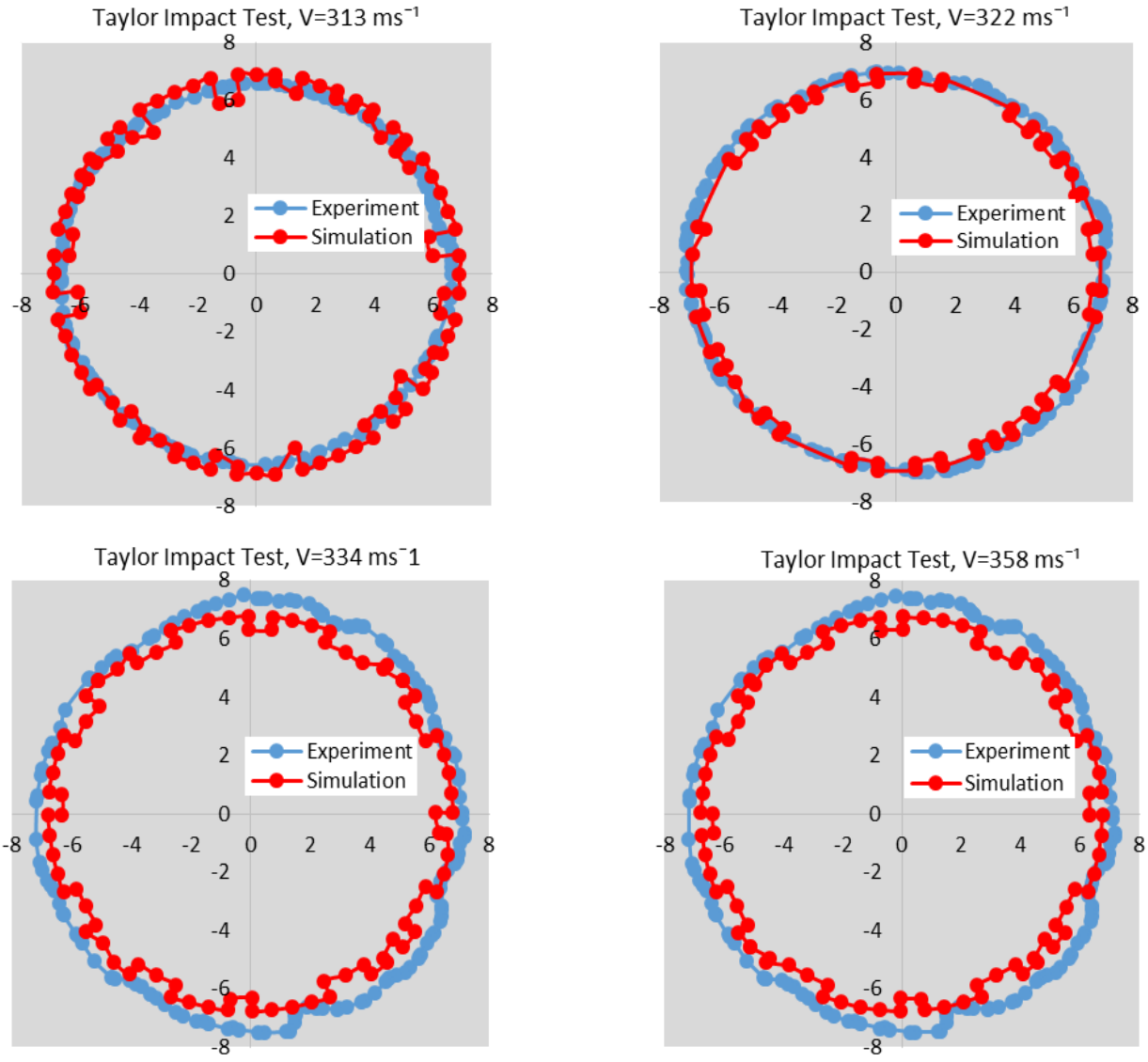

Fig. 13. Simulation of the Petalling Fracture Mode

Table 6
Comparison between Experiment and Numerical Results of the Taylor Impact Test

Impact velocity (m/s)	Data	Final length after impact (mm)	Final diameter after impact (mm)
191	Experimental	13.55	10.36
	Simulation	13.02	10.35
	Percentage error (%)	3.90	0.10
209	Experimental	13.05	10.39
	Simulation	12.73	10.42
	Percentage error (%)	2.45	0.30
220	Experimental	12.80	10.73
	Simulation	12.51	10.93
	Percentage error (%)	2.27	1.86
231	Experimental	12.45	10.84
	Simulation	12.70	11.14
	Percentage error (%)	2.00	2.77
280	Experimental	12.15	11.27
	Simulation	11.80	12.51
	Percentage error (%)	2.88	11.00
295	Experimental	11.95	13.30
	Simulation	11.43	12.47
	Percentage error (%)	4.35	6.24
313	Experimental	11.75	13.25
	Simulation	10.95	13.72
	Percentage error (%)	6.81	3.55
322	Experimental	11.28	14.13
	Simulation	10.73	13.79
	Percentage error (%)	4.88	2.41
334	Experimental	10.85	14.34
	Simulation	10.50	12.67
	Percentage error (%)	3.23	11.65
358	Experimental	10.65	14.34
	Simulation	9.77	12.75
	Percentage error (%)	8.26	11.09

In general, the numerical model can predict the elastoplastic deformation behaviour of the recycled aluminium alloy AA6061 reinforced with alumina oxide at a higher strain rate. The input parameters were successfully validated, and the comparison with the experimental data showed satisfactory agreement for each test.

3. Conclusions

The input parameters of the Simplified Johnson-Cook model (MAT 98) for recycled aluminium alloy AA6061 reinforced with alumina oxide were successfully characterised. The simulation results were validated against experimental data from the uniaxial tensile test and the Taylor cylinder impact test. The Simplified Johnson-Cook model (MAT 98) successfully predicts the elastoplastic behaviour of recycled aluminium alloy AA6061 reinforced with alumina oxide in uniaxial tensile tests. Simulation results showed good agreement with experimental data at various strain rates ranging from quasi-static to intermediate. As the strain rate increased, the flow stress increased. Simulation values for Young's modulus, yield strength, and ultimate tensile strength also agreed with experimental values, with acceptable percentage errors.

A similar simplified Johnson-Cook model is used for the Taylor cylinder impact test (MAT 98). The numerical model of the Taylor cylinder impact test can predict the mushrooming fracture mode from the initial impact velocity to the critical impact velocity. However, compared with the experimental data, this model cannot provide better prediction for other fracture modes. After the damage parameters of primary aluminium alloy AA6061 are included in the numerical model, the model can predict the simulation result of Taylor cylinder impact test and show good agreement with the experimental results for the critical impact velocity and the highest impact velocity. It was found that the damage parameters of the primary aluminium alloy AA6061 could be used for the recycled counterpart, demonstrating the ability of the numerical model to represent the evolution of anisotropy. The model successfully predicted the fracture modes of mushrooming, tensile splitting, and petalling fracture modes, similar to the experimental observations. The simulation results agree with the experimental data in terms of fracture mode, final length, and footprint with acceptable percent errors.

Based on these analyses, the Simplified Johnson-Cook model including damage parameters were able to predict the deformation behaviour of the recycled aluminium alloy AA6061 reinforced alumina oxide from the quasi-static state to high strain rates, including the fracture mode. These results contribute to the understanding of material behaviour and provide valuable insight for future design and analysis in similar applications. Despite the positive result, much research remains to be done to verify the anisotropic behaviour of such materials and to determine input parameters for predicting excellent results in simulation.

Acknowledgement
Authors wish to convey sincere gratitude to the Ministry of Higher Education Malaysia (MOHE) for providing the financial means during the preparation to complete this work under Fundamental Research Grant Scheme (FRGS/1/2020/TK02/UTHM/02/5), FRGS Vot K331.

References

[1] Hassan, Mohd Nasir, Theng Lee Chong, Md Mizanur Rahman, Mohd Nazeri Salleh, Z. Zakariah, Muhamad Awang, and M. N. Yunus. "Solid waste management–what's the Malaysian position." In *Seminar on Waste to Energy*. Malaysia: University Putra Malaysia, 2000. https://doi.10.22452/mjem.02.1.03

[2] Yusuf, Nur Kamilah. "A new approach of direct recycling of aluminium alloy chips (AA6061) in hot press forging process." PhD diss., Universiti Tun Hussein Malaysia, 2013.

[3] Ab Rahim, S. N., M. A. Lajis, and S. Ariffin. "A review on recycling aluminum chips by hot extrusion process." *Procedia CIRP* 26 (2015): 761-766. https://doi.org/10.1016/j.procir.2015.01.013

[4] Tillová, Eva, Mária Chalupová, and Lenka Hurtalová. "Evolution of phases in a recycled Al-Si cast alloy during solution treatment." In *Scanning electron microscopy*. IntechOpen, 2012. https://doi.org/10.5772/34542

[5] Das, Subodh K. "Designing aluminium alloys for a recycling friendly world." In *Materials Science Forum*, vol. 519, pp. 1239-1244. Trans Tech Publications Ltd, 2006. https://doi.10.4028/www.scientific.net/MSF.519-521.1239

[6] Hemanth, Joel. "Development and property evaluation of aluminum alloy reinforced with nano-ZrO2 metal matrix composites (NMMCs)." *Materials Science and Engineering: A* 507, no. 1-2 (2009): 110-113. https://doi.org/10.1016/j.msea.2008.11.039

[7] Feng, C. F., and Ludo Froyen. "Formation of Al3Ti and Al2O3 from an Al–TiO2 system for preparing in-situ aluminium matrix composites." *Composites Part A: Applied Science and Manufacturing* 31, no. 4 (2000): 385-390. https://doi.org/10.1016/S1359-835X(99)00041-X

[8] Ramesh, M., T. Karthikeyan, and A. Kumaravel. "EFFECT OF REINFORCEMENT OF NATURAL RESIDUE (QUARRY DUST) TO ENHANCE THE PROPERTIES OF ALUMINIUM METAL MATRIX COMPOSITES." *Journal of Industrial Pollution Control* 30, no. 1 (2014). https://doi.10.5958/j.0974-0910.30.1.017

[9] Ghandva, Hamidreza, Saif Yasir Ali, and Muhamad Azizi Mat Yajid. "Effect of Gd Addition on Microstructural and Mechanical Properties of Al-18% Si Alloy for Automotive Applications." *Journal of Advanced Research in Applied Mechanics* 87, no. 1 (2021): 1-10.

[10] Ramli, Rosmamuhamadani, Nabila Nujaimi Ab Basir, Noor Amira Ramlan, Nur Fathiah Mohd Razali, Mohd Muzamir Mahat, Syaiful Osman, and Sabrina M. Yahaya. "Characterization of Aluminium-Magnesium (Al-Mg) Alloy Reinforced with Strontium (Sr) by Casting Technique." *Journal of Advanced Research in Applied Mechanics* 103, no. 1 (2023): 27-32. https://doi.org/10.37934/aram.103.1.2732

[11] Hamdan, Hasanudin, Nadlene Razali, Anita Akmar Kamarolzaman, Nurfaizey Abdul Hamid, Siti Hajar Sheikh Md Fadzullah, Emy Aqillah Sharif, Syazwan Ahmad Rashidi, and Sarah Othman. "Characterization of Carbon Fibre Reinforced Polyphenylene Sulfide Composite Under Interlaminar Shear Strength." *Journal of Advanced Research in Applied Mechanics* 102, no. 1 (2023): 1-9. https://doi.org/10.37934/aram.102.1.19

[12] Chen, Y., A. H. Clausen, O. S. Hopperstad, and M. Langseth. "Stress–strain behaviour of aluminium alloys at a wide range of strain rates." *International Journal of Solids and Structures* 46, no. 21 (2009): 3825-3835. https://doi.org/10.1016/j.ijsolstr.2009.07.013

[13] Abdul Latif, Noradila, Zainuddin Sajuri, Syarif Junaidi, Yukio Miyashita, and Yoshiharu Mutoh. "Effect of strain rate on tensile and work hardening properties for Al-Zn magnesium alloys." *International Journal of Materials Engineering Innovation* 5, no. 1 (2014): 28-37. https://doi.org/10.1504/IJMATEI.2014.059487

[14] Bogusz, Anna, and Mirosława Bukowska. "Stress-strain characteristics as a source of information on the destruction of rocks under the influence of load." *Journal of Sustainable Mining* 14, no. 1 (2015): 46-54. https://doi.org/10.1016/j.jsm.2015.08.007

[15] Wicaksana, Y., and S. Jeon. "Strain rate effect on the crack initiation stress level under uniaxial compression." In *9th Asian Rock Mechanics Symposium*, pp. 1-9. 2016.

[16] Ho, C. S., and M. K. Mohd Nor. "Tensile behaviour and damage characteristic of recycled aluminium alloys AA6061 undergoing finite strain deformation." *Proceedings of the Institution of Mechanical Engineers, Part C: Journal of Mechanical Engineering Science* 235, no. 12 (2021): 2276-2284. https://doi.org/10.1177/0954406220950349

[17] Ma'at, Norzarina, Mohd Khir Mohd Nor, Choon Sin Ho, Noradila Abdul Latif, Kamarul-Azhar Kamarudin, Saifulnizan Jamian, Mohd Norihan Ibrahim, and Muhamad Khairudin Awang. "Effects of Temperatures and Strain Rate on the Mechanical Behaviour of Commercial Aluminium Alloy AA6061." *Journal of Advanced Research in Fluid Mechanics and Thermal Sciences* 54, no. 1 (2019): 21-26. https://doi.10.37934/arfmts.54.1.2126

[18] Mohd Nor, Mohd Khir, and Ibrahim Mohamad Suhaimi. "Effects of temperature and strain rate on commercial aluminum alloy AA5083." *Applied Mechanics and Materials* 660 (2014): 332-336. https://doi.10.4028/www.scientific.net/AMM.660.332

[19] Panov, Vili. "Modelling of behaviour of metals at high strain rates." (2006). https://doi.org/10.1063/1.2263405

[20] Lim, Hojun, Jay D. Carroll, Corbett C. Battaile, Shuh Rong Chen, Alexander P. Moore, and J. Matthew D. Lane. "Anisotropy and strain localization in dynamic impact experiments of tantalum single crystals." *Scientific reports* 8, no. 1 (2018): 5540. https://doi.10.1038/s41598-018-34844-6

[21] Sen, Subhajit, Biswanath Banerjee, and Amit Shaw. "Taylor impact test revisited: Determination of plasticity parameters for metals at high strain rate." *International Journal of Solids and Structures* 193 (2020): 357-374. https://doi.10.1016/j.ijsolstr.2020.02.020

[22] Li, Jun-Cheng, Gang Chen, Feng-Lei Huang, and Yong-Gang Lu. "Load characteristics in Taylor impact test on projectiles with various nose shapes." *Metals* 11, no. 5 (2021): 713. https://doi.org/10.3390/met11050713

[23] Ho, C. S., and M. K. Mohd Nor. "An experimental investigation on the deformation behaviour of recycled aluminium alloy AA6061 undergoing finite strain deformation." *Metals and Materials International* 27 (2021): 4967-4983. https://doi.org/10.1007/s12540-020-00858-8

[24] Ho, Choon Sin, Muhamad Afandi Ab Rani, Mohd Khir Mohd Nor, Norzarina Ma'at, Mohamed Thariq Haji Hameed Sultan, Mohd Amri Lajis, and Nur Kamilah Yusuf. "Characterization of anisotropic damage behaviour of recycled aluminium alloys AA6061 undergoing high velocity impact." *International Journal of Integrated Engineering* 11, no. 1 (2019). https://doi.org/10.11113/ijie.v4.n3.195

[25] Maat, Norzarina, Mohd Khir Mohd Nor, and Choon Sin Ho. "Characterisation of Mechanical Properties, Damage Progression and Fracture Modes of Recycled Aluminium Alloys AA6061 Reinforced Alumina Oxide." *International Journal of Integrated Engineering* 13, no. 7 (2021): 215-225. https://doi.10.30880/ijie.2021.13.07.028

[26] Ma'at, N., C. S. Ho, MK Mohd Nor, and MT Hameed Sultan. "High Strain Rate Deformation Behaviour Analysis of Recycled Aluminium Alloys AA6061 Reinforced Alumina Oxide Al2O3 Using Taylor Cylinder Impact Test." (2022). https://doi.10.15282/jmes.11.si1.2022.19.0671

[27] Hosseinpour, F., and H. Hajihosseini. "Importance of simulation in manufacturing." *World Academy of Science, Engineering and Technology* 51, no. 3 (2009): 292-295.

[28] Mohd Nor, Mohd Khir, Rade Vignjevic, and James Campbell. "Modelling of shockwave propagation in orthotropic materials." *Applied Mechanics and Materials* 315 (2013): 557-561. https://doi.10.4028/www.scientific.net/AMM.315.557

[29] Elmarakbi, A. M., Ning Hu, and Hisao Fukunaga. "Finite element simulation of delamination growth in composite materials using LS-DYNA." *Composites Science and Technology* 69, no. 14 (2009): 2383-2391. https://doi.org/10.1016/j.compscitech.2009.01.036
[30] Nor, MK Mohd. "Modeling of constitutive model to predict the deformation behaviour of commercial aluminum alloy AA7010 subjected to high velocity impacts." *ARPN J. Eng. Appl. Sci* 11, no. 4 (2016): 2349-2353.
[31] Mohd Nor, M. K., C. S. Ho, N. Ma'at, and M. F. Kamarulzaman. "Modelling shock waves in composite materials using generalised orthotropic pressure." *Continuum mechanics and thermodynamics* 32 (2020): 1217-1229. https://doi.org/10.1007/s00161-019-00835-6
[32] Wekezer, Jerry W., and Krzysztof Cichocki. "Application of LS-DYNA in Numerical Analysis of Vehicle Trajectories." In *Proceedings ouf 7t International LS-DYNA Users' Conference, Dearborn*. 2002.
[33] Valayil, Tony Punnoose, and Jason Cherian Issac. "Crash simulation in ANSYS LS-DYNA to explore the crash performance of composite and metallic materials." *International Journal of Scientific & Engineering Research* 4, no. 8 (2013).
[34] Mohd Nor, Mohd Khir, and Muhammad Zulhusmi Dol Baharin. "Rollover analysis of heavy vehicle bus." *Applied Mechanics and Materials* 660 (2014): 633-636. https://doi.org/10.4028/www.scientific.net/amm.660.633
[35] Murugesan, Mohanraj, and Dong Won Jung. "Johnson Cook material and failure model parameters estimation of AISI-1045 medium carbon steel for metal forming applications." *Materials* 12, no. 4 (2019): 609. https://doi.org/10.3390/ma12040609
[36] HADDOU, Mounir El Yakhloufi. "Modeling of Damage Evolution and Fracture in 5182 H111 Aluminum Alloy." *Journal of Sustainable Construction Materials and Technologies* 1, no. 1: 23-28. https://doi.10.29187/jscmt.2017.2
[37] Banerjee, A., S. Dhar, S. Acharyya, D. Datta, and N. Nayak. "Determination of Johnson cook material and failure model constants and numerical modelling of Charpy impact test of armour steel." *Materials Science and Engineering: A* 640 (2015): 200-209. https://doi.org/10.1016/j.msea.2015.05.073
[38] Kruszka, Leopold, J. Janiszewski, and M. Grązka. "Experimental and numerical analysis of Al6063 duralumin using Taylor impact test." In *EPJ Web of Conferences*, vol. 26, p. 01062. EDP Sciences, 2012. https://doi.10.1051/epjconf/20122601062
[39] Majzoobi, G. H., and F. Rahimi Dehgolan. "Determination of the constants of damage models." *Procedia Engineering* 10 (2011): 764-773. https://doi.org/10.1016/j.proeng.2011.04.127
[40] Zhao, Jingwei, Hua Ding, Wenjuan Zhao, Mingli Huang, Dongbin Wei, and Zhengyi Jiang. "Modelling of the hot deformation behaviour of a titanium alloy using constitutive equations and artificial neural network." *Computational Materials Science* 92 (2014): 47-56. https://doi.org/10.1016/j.commatsci.2014.05.040
[41] Ashtiani, HR Rezaei, and A. A. Shayanpoor. "New constitutive equation utilizing grain size for modeling of hot deformation behavior of AA1070 aluminum." *Transactions of Nonferrous Metals Society of China* 31, no. 2 (2021): 345-357. https://doi.org/10.1016/S1003-6326(21)65500-0
[42] Churyumov, Alexander, Alena Kazakova, and Tatiana Churyumova. "Modelling of the steel high-temperature deformation behaviour using artificial neural network." *Metals* 12, no. 3 (2022): 447. https://doi.org/10.3390/met12030447
[43] Cho, Jeongho, and Shin-Hyung Song. "Modeling hot deformation of 5005 aluminum alloy through locally constrained regression models with logarithmic transformations." *Applied Sciences* 12, no. 1 (2021): 152. https://doi.org/10.3390/app12010152
[44] Akram, Sohail, Syed Husain Imran Jaffery, Mushtaq Khan, Muhammad Fahad, Aamir Mubashar, and Liaqat Ali. "Numerical and experimental investigation of Johnson–Cook material models for aluminum (Al 6061-T6) alloy using orthogonal machining approach." *Advances in Mechanical Engineering* 10, no. 9 (2018): 1687814018797794. https://doi.org/10.1177/1687814018797794